Protein Science (1997), *6*:399–406. Cambridge University Press. Printed in the USA.

Conformational stability of pGEX-expressed *Schistosoma japonicum* glutathione S-transferase: A detoxification enzyme and fusion-protein affinity tag

WARREN KAPLAN,[1] PAUL HÜSLER,[2] HORST KLUMP,[2] JULIJA ERHARDT,[1] NICOLAS SLUIS-CREMER,[1] AND HEINI DIRR[1]

[1]Protein Structure–Function Research Programme, Department of Biochemistry, University of the Witwatersrand, Johannesburg 2050, South Africa
[2]Department of Biochemistry, University of Cape Town, Private Bag, Rondebosch 7700, South Africa

(RECEIVED September 9, 1996; ACCEPTED November 19, 1996)

Abstract

A glutathione S-transferase (Sj26GST) from *Schistosoma japonicum*, which functions in the parasite's Phase II detoxification pathway, is expressed by the Pharmacia pGEX-2T plasmid and is used widely as a fusion-protein affinity tag. It contains all 217 residues of Sj26GST and an additional 9-residue peptide linker with a thrombin cleavage site at its C-terminus. Size-exclusion HPLC (SEC-HPLC) and SDS-PAGE studies indicate that purification of the homodimeric protein under nonreducing conditions results in the reversible formation of significant amounts of 160-kDa and larger aggregates without a loss in catalytic activity. The basis for oxidative aggregation can be ascribed to the high degree of exposure of the four cysteine residues per subunit. The conformational stability of the dimeric protein was studied by urea- and temperature-induced unfolding techniques. Fluorescence-spectroscopy, SEC-HPLC, urea- and temperature-gradient gel electrophoresis, differential scanning microcalorimetry, and enzyme activity were employed to monitor structural and functional changes. The unfolding data indicate the absence of thermodynamically stable intermediates and that the unfolding/refolding transition is a two-state process involving folded native dimer and unfolded monomer. The stability of the protein was found to be dependent on its concentration, with a $\Delta G°(H_2O) = 26.0 \pm 1.7$ kcal/mol. The strong relationship observed between the *m*-value and the size of the protein indicates that the amount of protein surface area exposed to solvent upon unfolding is the major structural determinant for the dependence of the protein's free energy of unfolding on urea concentration. Thermograms obtained by differential scanning microcalorimetry also fitted a two-state unfolding transition model with values of $\Delta C_p = 7{,}440$ J/mol per K, $\Delta H = 950.4$ kJ/mol, and $\Delta S = 1{,}484$ J/mol.

Keywords: aggregation; conformational stability; denaturation; glutathione S-transferase; unfolding

The homodimeric (26 kDa/subunit) glutathione S-transferase (EC2.5.1.18) from *Schistosoma japonicum* (Sj26GST) catalyses the S-conjugation between the thiol group of glutathione and an electrophilic moiety of xenobiotic and endobiotic toxic compounds (Armstrong, 1991). Sj26GST is a member of one of the most important supergene family of enzymes involved in the Phase II metabolism of electrophilic compounds (Armstrong, 1991). The glutathione-conjugates have greater solubility in water, facilitating their export from the cell, where they are metabolized via the mercapturate pathway and eventually excreted. Sj26GST is also a nonsubstrate ligand-binding protein capable of sequestering host-derived heme in the parasitic helminth, thus reducing heme-induced oxidative damage and the formation of toxic haematin crystals (Smith et al., 1986; McTigue et al., 1995).

Sj26GST first drew attention when it was identified by Smith et al. (1986) as a major antigen capable of inducing host-protective immunity in mice. The fact that it could be purified easily in large amounts using glutathione affinity chromatography led to the development of the pGEX gene fusion expression system, which expresses the fully functional and highly soluble Sj26GST (Smith & Johnson, 1988). Today, the pGEX system is used widely for the overexpression in *Escherichia coli* of a wide variety of proteins

Reprint requests to: H. Dirr, Protein Structure–Function Research Programme, Department of Biochemistry, University of the Witwatersrand, Johannesburg 2050, South Africa; e-mail: 089dirr@cosmos.wits.ac.za.

Abbreviations: CDNB, 1-chloro-2,4-dinitro-benzene; DSC, differential scanning calorimetry; DTNB, dithionitrobenzene; DTT, dithiothreitol; GSH, reduced glutathione; GST, glutathione S-transferase; PBS, phosphate-buffered saline; SEC-HPLC, size-exclusion high performance liquid chromatography; Sj26GST, 26-kDa glutathione S-transferase from *Schistosoma japonicum*; TGGE, thermal gradient gel electrophoresis; UGGE, urea gradient gel electrophoresis.

fused to the C-terminus of Sj26GST (LaVallie & McCoy, 1995). Furthermore, the dimeric structure of Sj26GST with C-terminus fusion proteins has also led to some interesting structure–function studies such as mimicry of receptor dimerization (Yan et al., 1995), and the identification of oligomeric structures of proteins (Nemoto et al., 1995). Overexpressed Sj26GST, however, is inclined to undergo oxidative aggregation, which impairs the proteolytic removal of the fusion protein from Sj26GST (Abeliovich & Shlomai, 1995).

Crystal structures of Sj26GST have been solved for the apoenzyme form (McTigue et al., 1995), and for complexes with either the physiological substrate glutathione (GSH) (Lim et al., 1994) or with the nonsubstrate ligand and major antischistosomal drug praziquantel (PZQ) (McTigue et al., 1995). The protein shares the archetypical fold with other members of the GST family (Dirr et al., 1994), and the binding of substrate or nonsubstrate ligands does not significantly change the protein's conformation. Each subunit in homodimeric Sj26GST contains two structural domains (Lim et al., 1994); an N-terminus domain (domain I) with a $\beta\alpha\beta\alpha\beta\beta\alpha$ folding topology (residues 1–84), and a C-terminus all-α-helical domain (domain II; residues 85–217) (residues are numbered according to Lim et al., 1994). The dimeric structure is required for the formation of two functional active sites (one per subunit) and a nonsubstrate ligand binding site at the dimer twofold axis. Dimerization also appears to be essential for maintaining thermodynamically stable and functional GST structures (Dirr & Reinmer, 1991; Kong et al., 1993; Erhardt & Dirr, 1995). The helminth GST is a class mu GST (and not class sigma as suggested by some) on the basis of sequence homologies, structural similarities, conserved G-sites, and class-specific molecular recognition at the subunit interface. Regarding the latter, the class mu interface is more hydrophobic than the sigma interface and it has a prominent "lock-and-key" type hydrophobic interaction at the subunit interface, a feature that is conserved in the alpha/mu/pi classes, but that is absent in class sigma and class theta enzymes (Ji et al., 1992, 1995; Lim et al., 1994; McTigue et al., 1995; Wilce et al., 1995; Reinemer et al., 1996). A class mu isoenzyme (rGSTM1-1) also has been used successfully as a search model in the molecular replacement solution of the Sj26GST structure (Lim et al., 1994).

GST-fusions can also be used to crystallize peptide or protein fragments and for phasing fusion-protein structures by Patterson search methods (Carter et al., 1994; Lim et al., 1994).

In light of the physiological importance of the Sj26GST as a detoxification protein and vaccine and drug target, and its wide application in protein biotechnology, this paper describes the first conformational stability study for the parasitic helminth GST in order to understand more clearly its conformational dynamics and subunit folding and assembly.

Results

Aggregation of Sj26GST under nonreducing conditions

Sj26GST, as expressed by the pGEX-2T plasmid, has a tendency to undergo oxidative aggregation when extracted and purified under nonreducing conditions. SEC-HPLC elution profiles result in only the native dimeric Sj26GST when purified and analyzed in the presence of DTT. The absence of DTT results in a mixture of native protein together with 160-kDa and larger aggregates (40% native and 60% aggregates). Furthermore, SDS-PAGE in the absence of β-mercaptoethanol indicated the presence of a high molecular mass aggregate (at 73 kDa) in addition to the monomer (at 26 kDa) for protein not purified under reducing conditions (data not shown). All aggregates disappeared when DTT was present, indicating a reversible process. Comparable specific activities were obtained for both native dimeric (10.8 μmol/min/mg) and aggregated enzyme (9.4 μmol/min/mg). Sj26GST has four cysteine residues per subunit, none of which are involved in intrasubunit disulfide bonds (Lim et al., 1994; McTigue et al., 1995). Titration of the recombinant protein with DTNB yielded values of 3.5 and 3.7 free cysteines per subunit for folded protein and for unfolded protein, respectively.

Urea-induced unfolding/refolding

Reversibility of unfolding (structure and function)

To study unfolding under equilibrium conditions, it is necessary to show that the process is reversible (Pace et al., 1989). Tryptophan fluorescence and enzyme activity were used as structural and functional probes to monitor changes in the Sj26GST molecule during unfolding/refolding. The enzyme contains four tryptophan residues per subunit (Trp 7, Trp 40, Trp 200, and Trp 205). The tryptophan emission spectrum for the folded protein (excitation at 295 nm) has an emission maximum at 335 nm, which shifts to 355 nm when the protein unfolds. This red shift is accompanied by a large increase in quantum yield, suggesting that the tryptophan residues are located in a hydrophobic environment in the folded protein (Teal, 1960). Refolding of the denatured protein by a 10-fold dilution in nondenaturing buffer resulted in a blue shift from 355 nm to 335 nm. About 90% of the emission intensity at 335 nm was recovered when compared with untreated folded protein. Furthermore, the recovery of enzyme activity following refolding was in excess of 80%. The data indicate that refolding proceeds mainly to a catalytically functional conformation.

Unfolding transitions and protein concentration dependence

Enzyme activity and tryptophan fluorescence unfolding data resulted in coincident and monophasic unfolding curves (Fig. 1). The midpoint of the unfolding transition increased to higher urea concentration with increasing protein concentration (Fig. 1, insert). The monophasic and coincident transition curves for fluorescence and activity data and the protein concentration dependence of this data suggest a two-state unfolding/refolding model (Bowie & Sauer, 1989). This allowed us to estimate the conformational stability of the Sj26GST in the absence of denaturant; $\Delta G°(H_2O) = 26.0 \pm 1.7$ kcal/mol, and the m-value = 4.5 kcal/mol per M urea. The experimentally determined m-value compares well with a value of 4.92 kcal/mol per M urea calculated from (Myers et al., 1995):

$$m = 374 + 0.11(\Delta ASA)$$

where ΔASA is the change in solvent-accessible surface area upon unfolding ($\Delta ASA = -907 + 93\{\text{number of amino acid residues}\} = 41{,}129$ Å^2).

UGGE

Because certain conformational states might go undetected by spectroscopic probes (Creighton, 1986), we utilized UGGE to monitor changes in hydrodynamic volume to ascertain whether any intermediate conformational states were present along the unfolding/refolding pathway of Sj26GST. Figure 2 illustrates the electro-

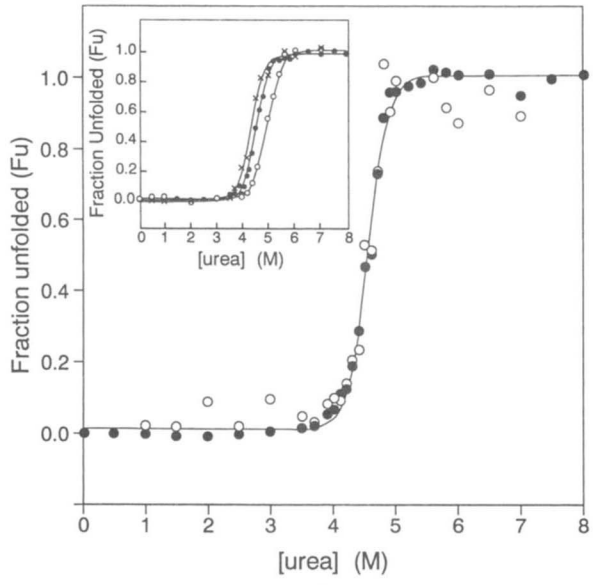

Fig. 1. Urea-unfolding curves for Sj26GST. Tryptophan fluorescence (○) and enzyme activity (●) were used to monitor the unfolding of 2 μM Sj26GST. The C_m value occurs at 4.5 M urea. Insert shows the protein-concentration dependence of Sj26GST stability against urea at 0.2 μM (×), 2 μM (●), and 20 μM (○).

phoretic behavior of the protein when applied across the gradient of urea in the folded state (Fig. 2A) and in the unfolded state (Fig. 2B). The protein bands in the two electrophoretograms are very similar, showing a single transition between 4 and 5 M urea. This transition corresponds with the urea unfolding data illustrated in Figure 1. The discontinuity between the bands of native and unfolded Sj26GST indicates that unfolding and refolding are relatively slow on the time scale of the electrophoresis near the transition midpoint (i.e., the two states are in slow equilibrium, allowing for their accumulation) (Mitchell, 1976; Creighton, 1986).

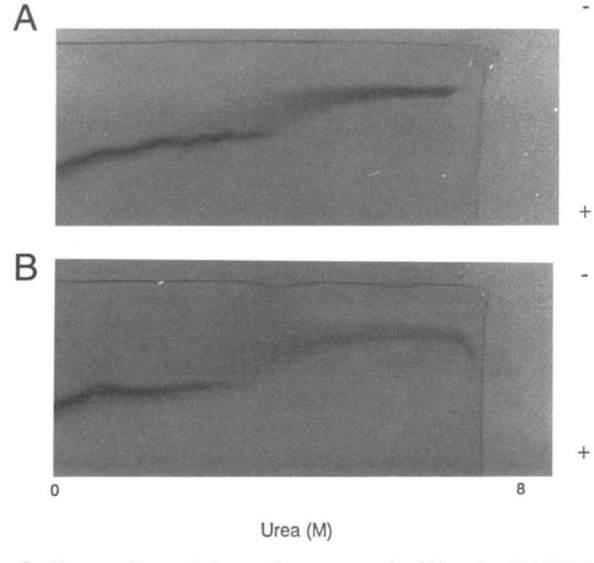

Fig. 2. Urea-gradient gel electrophoretograms for (**A**) native Sj26GST and (**B**) unfolded Sj26GST. The urea gradient (0–8 M) is perpendicular to the direction of electrophoresis from cathode to anode. Transition occurs between 4 and 5 M urea.

SEC-HPLC

SEC-HPLC is useful for studying protein folding/unfolding due to its ability to resolve changes in the hydrodynamic volumes of macromolecules and, therefore, to detect the presence of kinetically stable intermediate states provided that they are stable within the time scale of the chromatographic run (Corbett & Roche, 1984). Figure 3 shows elution profiles of sj26GST in the presence of increasing concentrations of urea. Only two molecular species are observed; one species at the retention time for the native dimeric protein, and the other at the retention time for the unfolded monomer. The midpoint of the unfolding transition appears at 4.85 M urea and is similar to the midpoint value obtained by tryptophan fluorescence (Fig. 1, insert; Fig. 2). Folded intermediates (e.g., folded monomer) were not observed.

Thermal unfolding

In addition to urea, heat was also used as a denaturant because proteins have been known to unfold differently in different denaturants (Timm & Neet, 1992; Morjana et al., 1993; Myers et al., 1995; Ward et al., 1995). Under all the conditions reported here, thermal denaturation of the protein was found to be irreversible.

Thermal inactivation of Sj26GST

The loss of enzyme activity of Sj26GST with increasing temperature is shown in Figure 4A. The midpoint of the transition (45–55 °C) occurs at about 51 °C. These data are similar to that reported for hGSTP1-1 ($T_m \sim 52$ °C) (Kong et al., 1993).

TGGE

TGGE was performed in order to trap any intermediates that may have occurred along the thermally induced unfolding pathway. The

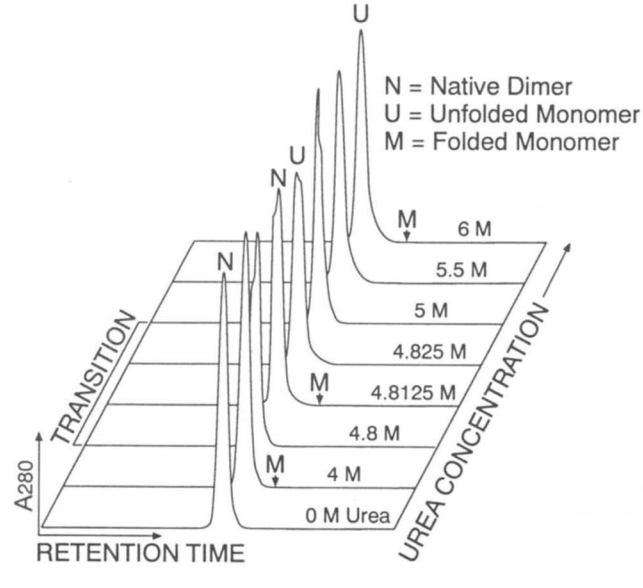

Fig. 3. SEC-HPLC elution profiles of Sj26GST with increasing concentrations of urea. Twenty-micromolar Sj26GST was incubated for 1 h at different concentrations of urea and applied to a SEC-HPLC column equilibrated with the same concentration of urea. The expected position of folded monomer if it had been observed is indicated by M.

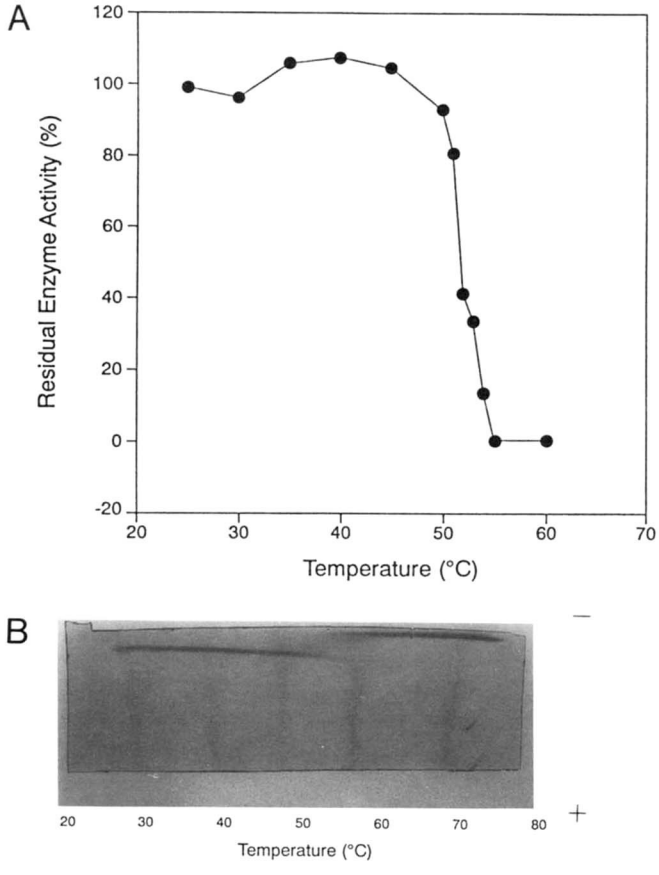

Fig. 4. Profile of decrease in enzyme activity (**A**) and thermal-gradient gel electrophoretogram (**B**) of Sj26GST. In A, 50 μg of the enzyme was incubated at each temperature for 10 min, and the remaining activity assayed in 0.1 M potassium phosphate buffer, pH 6.5, 1 mM GSH, 1 mM CDNB. Transition occurs between 45 and 55 °C. In B, native Sj26GST was electrophoresed through the gel with a linear thermal gradient from 20 to 80 °C perpendicular to the direction of electrophoresis, from cathode to anode. Transition occurs between 45 and 55 °C.

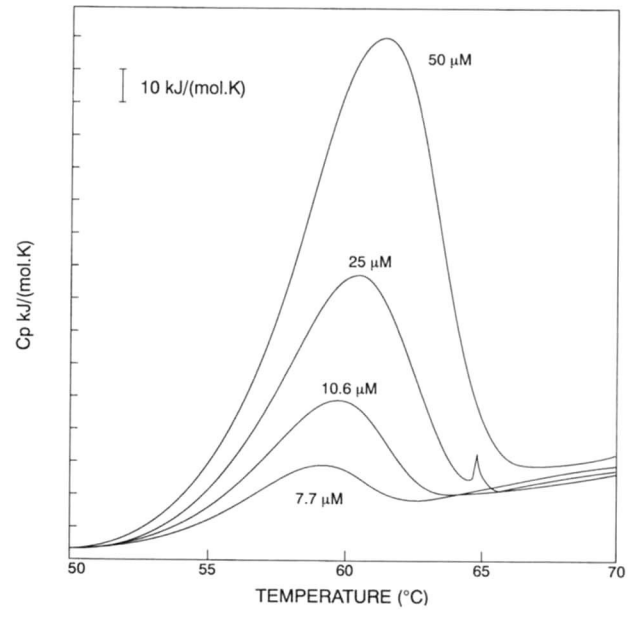

Fig. 5. DSC curves for Sj26GST at different protein concentrations (7.7–50 μM).

behavior of Sj26GST when electrophoresed across a temperature gradient (20–80 °C) is shown in Figure 4B and indicates a single transition between 45 and 55 °C. This corresponds with the inactivation data above. The discontinuity between the bands of native and unfolded Sj26GST indicates that unfolding is slow on the time scale of the electrophoresis near the transition midpoint, thus allowing for their accumulation. The protein band in the pretransitional region is nonparallel to the surface of application (top of gel) due to decreasing gel viscosity with increasing temperature (Birmes et al., 1990).

DSC

DSC has been used extensively as the most definitive technique for establishing the presence or absence of intermediate species along the unfolding pathway of macromolecules (for reviews, see Privalov & Potekhin, 1986; Sturtevant, 1987; Freire, 1994). The DSC curve for Sj26GST indicates that the protein unfolds in a single transition where T_m-values are dependent upon protein concentration (Fig. 5). In addition, the T_m values, as well as the shape of the curves, were independent of scan rate. Although the thermal denaturation of Sj26GST is an apparently irreversible process, and the interpretation of DSC data is based on reversible processes. The validity of applying equilibrium thermodynamics to irreversible processes has been indicated (Privalov, 1982; Sturtevant, 1987), provided that the T_m values of the excess heat capacity curves and their shapes are independent of scan rate (Freire et al., 1990; Sanchez-Ruiz, 1992), i.e., the denaturation process is not kinetically controlled. In the case of a strongly rate-limited, irreversible DSC transition, protein concentration effects may still be expected to occur if the dissociation of the native multimeric protein into monomers takes place before the rate-determining step, or if the kinetics of the irreversible process is not first order (Sanchez-Ruiz, 1992). Thereby implying that the existence of protein concentration dependence (in the absence of scan rate independence) does not provide evidence that the denaturation process is not kinetically controlled (Sanchez-Ruiz, 1992). Deconvolution of the curves indicates that the melting of Sj26GST is a two-state process (i.e., intermediates are present in negligible amounts). Table 1 lists the thermodynamic parameters derived from the fitted DSC scans.

The slope of a linear van't Hoff plot of $\ln(C_t)$ versus $1/T_m$ (where C_t is total protein concentration; Sturtevant, 1987) yields a $\Delta H_{vH} = 804$ kJ/mol. This is in reasonable agreement with $\Delta H_{cal} = 950$ kJ/mol (i.e., $r = \Delta H_{vH}/\Delta H_{cal} = 0.85$), supporting the assumption of a two-state process (Sturtevant, 1987).

Discussion

Oxidative aggregation of Sj26GST

Chemical modification (this study) and crystallographic data (Lim et al., 1994; McTigue et al., 1995) indicate the four cysteine residues per Sj26GST subunit to be highly exposed to solvent. The formation of intermolecular disulfide bonds involving some of these cysteines could, therefore, explain the oxidative aggregation observed for the protein as well as the reversal of aggregation by treatment with reducing agents. The four cysteines appear in domain II; Cys 84 is located near the subunit interface, whereas the

Table 1. *Table of thermodynamic parameters calculated from the fitted DSC data*

Concentration of Sj26GST (μM)	ΔH_{cal} (kJ/mol)	ΔH_{vH} (kJ/mol)	T_m (K)	ΔS (J/(mol·K))	ΔC_p (J/(mol·K))
50	921.7	960	334.4	1,441	5,170.8
25	933.3	990	333.4	1,457	10,965.1
10.6	995.9	968	332.6	1,555	6,196.1
Average	950.4	973	—	1,481	7,444
SD	±39.8	±15.9	—	±61.6	±3,092.2

other three residues are clustered together on the surface of domain II on the opposite side of the active site. Because none of the cysteines are situated near the active site, access to the sites is not affected by the oxidative association of dimers. Aggregated protein retains its ability to bind the affinity matrix and displays a specific activity comparable to that of the native dimeric protein. The close proximity of the clustered cysteines to the peptide linker (with thrombin cleavage site) fused to the C-terminus of Sj26GST provides an explanation for the reported obstruction of specific cleavage of GST-fusion proteins that have undergone oxidative aggregation (Abeliovich & Shlomai, 1995).

Unfolding/refolding model

It is reasonable to assume two basic models for the equilibrium unfolding/refolding pathway of Sj26GST. In model 1, active folded dimer (A_2), inactive folded monomer (A), and unfolded monomer (U) are significantly populated at equilibrium:

$$A_2 \overset{K_1}{\Leftrightarrow} 2A \overset{K_2}{\Leftrightarrow} 2U$$

where $K_1 = [A]^2/[A_2]$ is the equilibrium constant for the bimolecular dissociation reaction, and $K_2 = [U]/[A]$ is the equilibrium constant for the unimolecular unfolding reaction. The folded monomer is assumed to have a tertiary structure similar to that of the dimer subunit, but is catalytically inactive because the dimeric structure is required to form a fully functional active site (Dirr et al., 1994; Lim et al., 1994; McTigue et al., 1995).

In model 2, only active folded dimer (A) and unfolded monomer (U) are significantly populated:

$$A_2 \overset{K_u}{\Leftrightarrow} 2U$$

where $K_u = [U]^2/[A_2]$ is the equilibrium constant for the bimolecular reaction.

All experimental data presented in this study (i.e., the coincident structural and enzyme activity data, protein-concentration dependence, monophasic transitions, correlation between ΔH_{vH} and ΔH_{cal} data) support model 2, which describes a highly cooperative and concerted two-state pathway for the equilibrium unfolding/refolding of Sj26GST. The size of the protein or the amount of its surface area exposed to solvent upon unfolding is the major structural determinant for the m-value (Schellman, 1978; Alonso & Dill, 1991; Myers et al., 1995). The magnitude of the m-value is also indicative of a highly cooperative two-state unfolding/refolding process (Pace, 1986). The fact that a folded monomeric state was not detected at any stage indicates that it is thermodynamically unstable. This implies that the interactions at the subunit interface of the homodimeric protein are important for stabilizing the tertiary structure of the individual monomers. Molecular recognition for dimerization of the different types of GST monomers is strictly gene class specific (i.e., no interclass dimers are found). As in all other GST structures, intersubunit contacts in the Sj26GST dimer are formed primarily between domain I of one subunit and domain II of the other. The interface has extensive hydrophobic patches at either end and is hydrophilic near the dimer twofold axis. Dimerization creates a solvent-accessible cleft along the twofold that has been shown to function as a nonsubstrate binding site (McTigue et al., 1995). The most prominent hydrophobic interaction at the interface is the anchoring of the phenyl ring of Phe 51, located in a loop after α-helix 2 in domain I of one subunit, into a hydrophobic pocket between α-helix 4 and α-helix 5 in domain II of the adjacent subunit. This lock-and-key feature is also conserved at the dimer interface of class alpha/mu/pi enzymes, but is absent at the more hydrophilic interface in sigma and theta class dimers. Similarities observed in the unfolding and conformational stability data for Sj26GST and other isoenzymes with an alpha/mu/pi-type subunit interface (Dirr et al., 1994; Ji et al., 1995), and differences observed between the two major subunit interface types (J. Stevens & H. Dirr, unpubl. results), further attest to the important role played by subunit interactions in GST stabilization. At this stage, however, the contribution of the individual interactions toward the conformational stability of GSTs is unknown.

The cytosolic GSTs do not undergo posttranslational modification (Yeh et al., 1995), making *E. coli* heterologous expression systems suitable for their overexpression. Cytosolic GSTs are highly soluble proteins and GST fusions can be used as a strategy for expressing large quantities of soluble protein. The high overexpression levels achieved for Sj26GST in *E. coli* indicate the foreign protein's ability to fold efficiently to a thermodynamically stable, proteolysis-resistant, and functional conformation in the bacterial intracellular environment. Sj26GST is also able to refold spontaneously in vitro with high yields to its native form by diluting the denaturant, suggesting that chaperones/foldases are not essential for folding/refolding. However, the formation of inclusion bodies (aggregates of incorrectly folded protein) has been reported for some GSTs (Ji et al., 1995) and GST fusions (Hartman et al., 1992; Frangioni et al., 1993). Low-temperature induction suppresses GST inclusion body formation (Hartman et al., 1992; Bader & Leisinger, 1994), possibly by decreasing the driving force for protein self-association, by slowing down the rate of GST synthesis, and by changing the folding kinetics. The presence of kinetic barriers (e.g., possibly the correct alignment of the two structural domains, subunit assembly, and/or *cis/trans* isomerization at active site Pro 55) could result in the accumulation and self-association of

folding intermediates resulting in the formation of inclusion bodies (Georgiou & Valax, 1996). Because Sj26GST (and all the other cytosolic GSTs) does not have disulfide bonds, a kinetic barrier due to disulfide bond isomerization can be excluded.

Materials and methods

Expression and purification of Sj26GST

The pGEX-2T plasmid (Pharmacia) was used to overexpress the Sj26GST in *E. coli* strain JM109 (Smith et al., 1986; Smith & Johnson, 1988). Once the cells had reached an optical density of 0.6–1.0 in Luria-Bertani culture medium containing 50 μg/mL ampicillin, isopropyl-β-D-thiogalactoside was added at a final concentration of 1 mM to induce overexpression of *Sj26GST*. After 4 h, the bacterial cells were pelleted, resuspended in a minimum volume of PBS containing 1% (v/v) Triton X-100 (with or without 2 mM DTT), and then lysed in an ethanol/dry ice bath via sonication. After collecting the supernatant by centrifugation, the overexpressed *Sj26GST* was purified in the absence or presence of 2 mM DTT by *S*-hexylglutathione affinity chromatography as described (Dirr et al., 1991). The purity and homogeneity of the protein was judged by SDS-PAGE under reducing and nonreducing conditions (Dirr et al., 1991; Sluis-Cremer & Dirr, 1995).

Determination of free thiols

Just prior to experimentation, Sj26GST was buffer exchanged on a PM-10 column (Pharmacia) (0.1 M Tris, 1 mM EDTA, pH 7.5) in order to remove any DTT. The number of free cysteines in native and denatured (8 M urea) Sj26GST were determined with DTNB as described by Dirr et al. (1991).

Enzyme activity assay

The catalytic activity of Sj26GST was determined spectrophotometrically at 340 nm and at room temperature by adding enzyme to a reaction mixture containing 1 mM CDNB and 1 mM reduced GSH in 0.1 M sodium phosphate buffer, pH 6.5, containing 1 mM EDTA and 0.02% NaN_3. The linear progress curves were corrected for the corresponding nonenzymatic controls. In the unfolding studies with urea, the reactivation of unfolded enzyme was negligible under these conditions.

Fluorescence measurements

All fluorescence measurements were made at a constant room temperature of 23 °C using a Hitachi model 850 fluorescence spectrophotometer. The excitation band width was set to 5 nm and the emission band width to 10 nm. Samples were excited at 295 nm for measuring tryptophan fluorescence.

Unfolding/refolding studies

All unfolding/refolding experiments were performed at room temperature in 20 mM sodium phosphate buffer, pH 6.5, containing 0.1 M NaCl, 1 mM EDTA, 2 mM DTT, 0.02% NaN_3. Final concentrations of dimeric sj26GST ranged from 0.2 to 20 μM. At the start of the studies, Sj26GST was confirmed to be dimeric and unaggregated by SEC-HPLC. Stock solutions of urea were prepared fresh according to Pace et al. (1989). In the unfolding experiments, protein was incubated in buffer with urea (0–8 M) for 1 h. In the refolding studies, unfolded protein (20 μM in 6 M urea) was diluted 10-fold with buffer without urea. All spectroscopic and enzyme activity measurements were performed after equilibrium was attained.

Conformational stability calculations

Denaturation curves were evaluated according to the linear extrapolation method (Pace, 1986) for dimeric proteins (Bowie & Sauer, 1989) as described elsewhere (Pace et al., 1989). Briefly, an equilibrium constant, K_D, was calculated at each point in the transition region of the denaturation curve (Bowie & Sauer, 1989; Timm & Neet, 1992):

$$K_D = 2P_t[f_d^2/(1 - f_d)],$$

where P_t is the concentration of protein monomer, and f_d the fraction of unfolded protein. A linear dependence of the Gibbs free energy of unfolding ($\Delta G_D = -RT \ln K_D$) on the denaturant concentration is assumed (Schellman, 1978):

$$\Delta G_D = \Delta G_D^{H_2O} - m[\text{denaturant}],$$

where $\Delta G_D^{H_2O}$ represents the difference in Gibbs free energy between the unfolded and folded protein in the absence of denaturant.

The conformational stability parameters were determined by iterative fitting of denaturation curves to the above equations using Sigma Plot (version 5.0, Jandel Scientific) employing a Levenberg Marquard least-squares algorithm.

UGGE

Urea gradient gels were prepared as described previously (Creighton, 1986). An inverse gradient of acrylamide was used to compensate for small effects of urea on the electrophoretic mobilities of both folded and unfolded proteins (Creighton, 1979). Gels were pre-electrophoresed for 1 h at 20 mA, prior to adding 50 μg of protein. The sample was then electrophoresed for 3 h at 10 mA and the gels stained in Coomassie Brilliant Blue.

SEC-HPLC

The hydrodynamic volume of Sj26GST, at different urea concentrations (0–6 M), was measured at room temperature by analytical SEC-HPLC using a Tosohaas G2000SW or BioRad Bio-Sil SEC 250-5 column at a flow rate of 0.5 mL/min. All buffer solutions were degassed and filtered through a 0.45-micron nylon filter. Samples of 20 μM Sj26GST in different concentrations of urea were prepared 1 h before injecting onto the column, which was pre-equilibrated with the same concentration of denaturant. Elution profiles were recorded at 280 nm.

DSC

Calorimetric measurements were conducted on a differential scanning microcalorimeter model 4 (DASM-4; Mashpriborintork, Moscow), whose construction and principles of function have been described elsewhere (Privalov & Potekhin, 1986). Just prior to the DSC experiments, all Sj26GST samples were buffer exchanged on a PM-10 column (Pharmacia) with 20 mM sodium phosphate buffer,

pH 6.5, to remove DTT that interfered with the baseline. Final protein concentrations in the sample cell ranged from 7.7 to 50 μM. In order to check for scan rate independence, the heating rate of identical, but separate protein samples was varied, i.e., 0.5, 1, and 2 °C/min, and corrected for instrument dynamic response (Freire et al., 1990). Data were collected every 0.1 min and stored to disk for further processing. Instrument baselines were determined by scanning the heat capacity versus temperature with buffer in both reference and sample cells. Baselines were subtracted from the raw data before further analysis. Attempts at fitting the DSC curves to a multi-state reaction mechanism were abolished because the data fitted well to the following two-state reaction scheme:

$$F_{initial} \overset{K}{\Leftrightarrow} 2F_{final}$$

where K is the equilibrium constant, defined as a function of ΔH, ΔS, and the partial specific heat capacity, ΔC_p. The equilibrium constant can be expressed in terms of the Gibbs Helmholtz free energy as follows:

$$K = \exp(-\Delta G/RT), \tag{1}$$

$$\Delta G = \Delta H + \Delta C_p(T - T_R) - T\{\Delta S + \Delta C_p \ln(T/T_R) - R\ln(2C_t)\}. \tag{2}$$

Here, ΔH and ΔS are the enthalpy and entropy changes at reference temperatures T_R.

The enthalpy changes (ΔH_{cal}) were calculated by integrating ΔC_p versus temperature over the transition interval, taking the protein concentration into account. ΔC_p is the apparent heat capacity change from the initial state $F_{initial}$ to the final state F_{final}, and C_t is the protein concentration in molarity (M). The equilibrium constant K differs from a conventional equilibrium constant because the molar concentration term C_t has been included.

The molar enthalpy and entropy changes for the unfolding process were obtained by fitting Equations 3 and 4 to the experimental data.

$$\alpha_2 = (-K + (K^2 + 4K)^{1/2})/2. \tag{3}$$

Here α_2 is the fractional amount of species $F_{final} = \alpha_2 C_t$. The fitted molar heat capacity function (C_p), which represents the DSC data, can be expressed in terms of α_2, ΔH, and ΔC_p as follows:

$$C_p = \Delta H(d\alpha_2/dT) + \alpha_2 \Delta C_p. \tag{4}$$

T_m values were defined as

$$T_m = \Delta H/[\Delta S - R\ln(2C_t)], \tag{5}$$

where T_m is the midpoint of the transition, and R the gas constant (8.314 J/mol/K) ΔH_{vH} values at individual protein concentrations were calculated from the integrated ΔH_{cal} curves, where

$$\Delta H_{vH} = 6RT_m^2(d\alpha_2/dT), \tag{6}$$

where α is the first derivative of the fraction of the denatured protein.

TGGE

TGGE was performed as described previously by Birmes et al. (1990), with a 0.075 M boric acid/0.03 M borax buffer at pH 8.6 in a 30 × 30 × 0.1 cm vertical slab gel. Protein (250 μg) was added across the top of the gel and electrophoresed at a voltage of 50 V for 30 min in order to allow for the smooth application of the protein onto the gel. The voltage was then increased to 300 V for 2 h to allow for the uniform migration of the protein into the gel. Electrophoresis was then halted and a linear temperature gradient from 20 to 80 °C was established across the gel over 30 min. Electrophoresis was continued at 350 V for 5 h while maintaining the temperature gradient. Gels were stained with Coomassie Brilliant Blue.

Acknowledgments

We thank the Universities of the Witwatersrand and Cape Town, as well as the South African FRD for financial support.

References

Abeliovich H, Shlomai J. 1995. Reversible oxidative aggregation obstructs specific proteolytic cleavage of glutathione S-transferase fusion proteins. *Anal Biochem 228*:351–354.

Alonso DOV, Dill KA. 1991. Solvent denaturation and stabilization of globular proteins. *Biochemistry 30*:5974–5985.

Armstrong RN. 1991. Glutathione S-transferases: Reaction mechanism, structure, and function. *Chem Res Toxicol 4*:131–140.

Bader R, Leisinger T. 1994. Isolation and characterization of the *Methylophilus sp.* strain DM 11 gene encoding dichloromethane dehalogenase/glutathione S-transferase. *J Bacteriol 176*:3466–3473.

Birmes A, Sättler A, Maurer K, Riesner D. 1990. Analysis of the conformational transitions of proteins by temperature-gradient gel electrophoresis. *Electrophor 11*:795–801.

Bowie JU, Sauer RT. 1989. Equilibrium dissociation and unfolding of the arc repressor dimer. *Biochemistry 28*:7139–7143.

Carter DC, Rüker F, Ho JX, Lim K, Keeling K, Gilliland GL, Ji X. 1994. Fusion proteins as alternate crystallization paths to difficult structure problems. *Protein Pept Lett 1*:175–178.

Corbett RJT, Roche RS. 1984. Use of high-speed size-exclusion chromatography for the study of protein folding and stability. *Biochemistry 23*:1888–1894.

Creighton TE. 1979. Electrophoretic analysis of the unfolding of proteins by urea. *J Mol Biol 129*:235–264.

Creighton TE. 1986. Detection of folding intermediates using urea-gradient electrophoresis. *Methods Enzymol 131*:156–172.

Dirr HW, Mann K, Huber R, Ladenstein R, Reinemer P. 1991. Class π glutathione S-transferase from pig lung. Purification, biochemical characterization, primary structure and crystallization. *Eur J Biochem 196*:693–698.

Dirr HW, Reinemer P. 1991. Equilibrium unfolding of class π glutathione S-transferase. *Biochem Biophys Res Commun 180*:294–300.

Dirr H, Reinemer P, Huber R. 1994. X-ray crystal structures of cytosolic glutathione S-transferases. Implications for protein architecture, substrate recognition and catalytic function. *Eur J Biochem 220*:645–661.

Erhardt J, Dirr H. 1995. Native dimer stabilizes the subunit tertiary structure of porcine class pi glutathione S-transferase. *Eur J Biochem 230*:614–620.

Frangioni JV, Neel BG. 1993. Solubilization and purification of enzymatically active glutathione S-transferase (pGEX) fusion proteins. *Anal Biochem 210*:179–187.

Freire E. 1994. Statistical thermodynamic analysis of differential scanning calorimetry data: Structural deconvolution of heat capacity function of proteins. *Methods Enzymol 240*:502–530.

Freire E, van Osdol WW, Mayorga OL, Sanchez-Ruiz JM. 1990. Calorimetrically determined dynamics of complex unfolding transitions in proteins. *Annu Rev Biophys Biophys Chem 19*:159–188.

Georgiou G, Valax P. 1996. Expression of correctly folded proteins in *Escherichia coli*. *Curr Opin Biotechnol 7*:190–197.

Hartman J, Daram P, Frizzell RA, Rado T, Benos DJ, Sorscher EJ. 1992. Affinity purification of insoluble recombinant fusion proteins containing glutathione S-transferase. *Biotechnol Bioeng 39*:828–832.

Ji X, von Rosenvinge EC, Johnson WW, Tomarev SI, Piatigorsky J, Armstrong RN, Gilliland GJ. 1995. Three dimensional structure, catalytic properties, and evolution of a sigma class glutathione S-transferase from squid. *Biochemistry 34*:5317–5328.

Ji X, Zhang P, Armstrong RN, Gilliland GL. 1992. The three dimensional structure of a glutathione S-transferase from mu gene class. Structural anal-

ysis of the binary complex of isoenzyme 3-3 and glutathione at 2.2 Å resolution. *Biochemistry 31*:10169–10184.

Kong KH, Inoue H, Takahashi K. 1993. Site-directed mutagenesis study on the roles of evolutionally conserved aspartic acid residues in human glutathione S-transferase P1-1. *Protein Eng 6*:93–99.

LaVallie ER, McCoy JM. 1995. Gene fusion expression systems in *Escherichia coli*. *Curr Opin Biotechnol 6*:501–506.

Lim K, Ho JX, Keeling K, Gilliland GL, Ji X, Rüker F, Carter DC. 1994. Three-dimensional structure of *Schistosoma japonicum* glutathione S-transferase fused with a six-amino acid conserved neutralizing epitope of gp41 from HIV. *Protein Sci 3*:2233–2244.

McTigue MA, Williams DR, Tainer JA. 1995. Crystal structure of a schistosomal drug and vaccine target: Glutathione S-transferase from *Schistosoma japonica* and its complex with the leading antischistosomal drug praziquantel. *J Mol Biol 246*:21–27.

Mitchell RM. 1976. The spatial distribution of moving macromolecules undergoing isomerization. *Biopolymers 15*:1717.

Morjana NA, McKeone BJ, Gilbert HF. 1993. Guanidine hydrochloride stabilization of a partially unfolded intermediate during the reversible denaturation of protein disulfide isomerase. *Proc Natl Acad Sci USA 90*:2107–2111.

Myers JK, Pace CN, Scholtz JM. 1995. Denaturant *m* values and heat capacity changes: Relation to changes in accessible surface areas of protein folding. *Protein Sci 4*:2138–2148.

Nemoto T, Ota M, Ohara-Nemoto Y, Kaneko M. 1995. Identification of dimeric structure of proteins by use of glutathione S-transferase-fusion expression system. *Anal Biochem 227*:396–399.

Pace CN. 1986. Determination and analysis of urea and guanidine hydrochloride denaturation curves. *Methods Enzymol 131*:266–280.

Pace CN, Shirley BA, Thomson JA. 1989. Measuring conformational stability of a protein. In: Creighton TE, ed. *Protein structure: A practical approach, 2nd edition*. Oxford, UK: IRL press at Oxford University Press. pp 311–330.

Privalov PL. 1982. Stability of proteins. Proteins which do not present a single cooperative system. *Adv Protein Chem 35*:1–104.

Privalov PL, Potekhin SA. 1986. Scanning microcalorimetry in studying temperature-induced changes in proteins. *Methods Enzymol 131*:4–51.

Reinemer P, Prade L, Hof P, Neuefeind T, Huber R, Zettl R, Palme K, Schell J, Koelln I, Bartunik HD, Bieseler B. 1996. Three-dimensional structure of glutathione S-transferase from *Arabidopsis thaliana* at 2.2 Å resolution: Structural characterization of herbicide-conjugating plant glutathione S-transferases and a novel active site architecture. *J Mol Biol 255*:289–309.

Sanchez-Ruiz JM. 1992. Theoretical analysis of Lumry-Eyring models in differential scanning calorimetry. *Biophys J 61*:921–935.

Schellman JA. 1978. Solvent denaturation. *Biopolymers 17*:1305–1322.

Sluis-Cremer N, Dirr H. 1995. Conformational stability of Cys 45-alkylated and hydrogen peroxide-oxidised glutathione S-transferase. *FEBS Lett 371*:94–98.

Smith DB, Davern KM, Board PG, Tiu WU, Garcia EG, Mitchell GF. 1986. Mr 26,000 antigen of *Schistosoma japonicum* recognized by resistant WEHI 129/J mice is a parasite glutathione S-transferase. *Proc Natl Acad Sci USA 83*:8703–8707.

Smith DB, Johnson KS. 1988. Single-step purification of polypeptides expressed in *Escherichia coli* as fusions with glutathione S-transferase. *Gene 67*:31–40.

Sturtevant JM. 1987. Biochemical applications of differential scanning calorimetry. *Annu Rev Phys Chem 38*:463–488.

Teal FWJ. 1960. The ultraviolet fluorescence of proteins in neutral solution. *Biochem J 76*:381–388.

Timm DE, Neet KE. 1992. Equilibrium denaturation studies of mouse beta-nerve growth factor. *Protein Sci 1*:236–244.

Ward LD, Matthews JM, Zhang JG, Simpson RJ. 1995. Equilibrium denaturation of recombinant murine interleukin-6: Effect of pH, denaturants, and salt on formation of folding intermediates. *Biochemistry 34*:11652–11659.

Wilce MCJ, Board PG, Feil SC, Parker MW. 1995. Crystal structure of a theta class glutathione transferase. *EMBO J 14*:2133–2143.

Yan H, Lim JTE, Contillo LG, Krolewski JJ. 1995. Glutathione S-transferase fusion proteins mimic receptor dimerization in permeabilized cells. *Anal Biochem 231*:455–458.

Yeh HI, Hsieh CH, Wang LY, Tsai SP, Hsu HY, Tam MF. 1995. Mass spectrometric analysis of rat liver cytosolic glutathione S-transferases: Modifications are limited to N-terminal processing. *Biochem J 308*:69–75.